

SINGLE AND CONTRA-ROTATION HIGH SPEED PROPELLERS:  
FLOW CALCULATION AND PERFORMANCE PREDICTION

P.W.C. Wong, M. Maina, C.R. Forsey, A.J. Bocci  
Aircraft Research Association Limited  
Bedford, U.K.

ABSTRACT

Theoretical aerodynamic methods suitable for propeller performance and flowfield predictions are discussed and compared with experiment. The methods discussed consist of an advanced strip theory and the Denton Euler method. Features of the methods relevant to high speed, highly disc loaded propellers are emphasised. Experiment and theory are shown to compare reasonably closely for various types of single rotation propellers. Illustrations of scale effect and the effect of blade deflection under load are included. Consideration is given to the different definitions of thrust in the experiment and their interpretation using the Denton method. Some of the problems arising in the validation and use of the methods for contra-rotation propellers are indicated.

NOTATION

$C_D$	Drag coefficient
$C_L$	Lift coefficient
$C_n$	Normal force coefficient
$C_p$	Power coefficient or pressure coefficient
$C_T$	Thrust coefficient
$J$	Advance ratio $J = \pi V / \omega R$
$M$	Forward Mach Number
$M_L$	Local Mach Number
$p$	Number of blades
$R$	Blade radius
$R_c$	Non-dimensional radius
$r$	Radial coordinate
$u_z, u_\theta$	Induced velocities in axial and swirl directions at the propeller disc plane
$v_n$	Velocity of wake filament normal to sheet surface
$V$	Forward velocity
$W$	Blade element onset flow velocity
$W_0$	Blade element helical velocity
$w$	Wake displacement velocity
$w_1$	Blade element aerodynamic velocity
$x/c$	Non-dimensional distance along chord
$z$	Axial coordinate, positive downstream
$\alpha$	Blade element effective incidence
$\Delta V$	Flowfield velocity perturbation due to spinner/nacelle in isolation
$\Gamma$	Wake vortex strength
$\eta$	Efficiency $\eta = JC_T / C_p$
$\phi$	Blade element onset flow angle
$\phi_0$	Blade element helix angle, or wake helix angle for light loading $\phi_0 = \tan^{-1}(V/\omega r)$
$\phi_2$	Wake helix angle for heavy loading, $\phi_2 = \tan^{-1}[(V+w)/\omega r]$
$\omega$	Angular velocity

Superscripts

F	Effects due to front blade
R	Effects due to rear blade

I. INTRODUCTION

A programme of theoretical and experimental work on propellers designed for cruise speeds typical of turbofan transport aircraft has been carried out in the UK in recent years. These propellers are characterised by relatively high blade number and disc loading and can be either single or contra-rotation. This paper is mainly concerned with the theoretical work, discussing aerodynamic methods which have been developed for such propellers and the validation and use of these methods for performance prediction. Steady blade flow conditions are assumed, corresponding to zero incidence with an axisymmetric spinner/nacelle and ignoring any forward effect of interaction of the propeller wake with an afterbody such as a wing. Most of the theoretical work discussed here has been carried out under contract to Dowty Rotol Ltd, with some support from the Department of Trade and Industry.

The methods may be classified into two types, wake and field methods. Wake methods provide a means of determining the onset flow at the blade, and this may be combined with blade element lift and drag data to give the radial loading and performance. The flow model adopted in such methods is very simplified but it is commonly thought that an acceptable performance prediction is given over a wide range of operating conditions, at least for conventional propellers. The accuracy for higher speed propellers is more open to question. The field methods were developed for such applications but are computer intensive, limited to attached flow conditions, and their validity for performance prediction is not well established. Further uncertainty arises in the contra-rotation case with both types of methods since it is necessary to include a circumferential averaging of the wake of the front rotor to ensure that the rear rotor operates in a steady flowfield. The accuracy of the methods is important for design and performance prediction purposes and this paper addresses some of the issues involved.

In section II, the classical wake model of Goldstein is discussed. This model forms the basis of the standard Lock/Goldstein strip theory, regularly used in propeller design. An advanced method based on this model has been developed at ARA, the new method having a number of features which have been introduced to deal with the characteristics of the types of propellers considered here. The field method used to predict the details of the three-dimensional flowfield for both single and contra-rotation cases is the Denton Euler code, as implemented at ARA, and this is described in section III. A selection of comparisons between experiment and theory is given in section IV. In section V, a description of the use of the methods for the analysis of experimental results for a single rotation propeller configuration is given together with some discussion of issues arising in the design of advanced contra-rotation blades.

## II. WAKE METHODS

### Strip Theory based on the Classical Wake Model

Propeller wake theory is based on the concept that the helical trailing vortex sheets shed by the rotating blades induce a velocity field which modifies the onset flow at the blades. The model assumed in the classical methods is the ideal wake, which comprises trailing vortex filaments forming a regular screw surface of pitch and radial loading distribution corresponding to minimum energy loss per unit time. Goldstein<sup>(1)</sup> considered the infinitely lightly loaded case, for which the wake vortex sheet geometry is consistent with the screw surface defined by the paths of the propeller blade elements. Such a screw surface, traced out by a four blade propeller moving forward with right-hand screw, is shown in Fig 1.

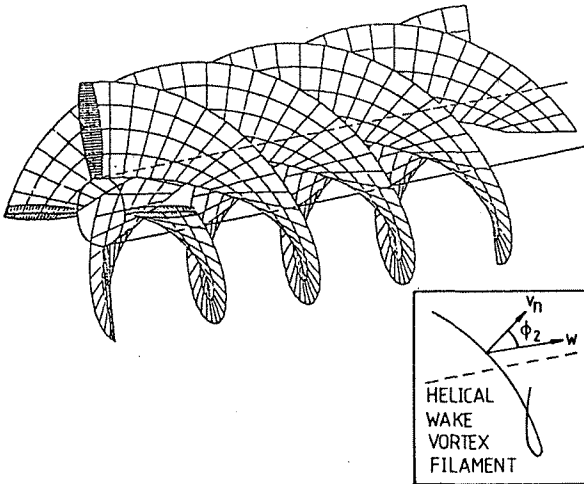


FIG. 1 PROPELLER SCREW SURFACES

Goldstein gave an exact solution for the incompressible potential flow between the wake surfaces for two and four blade cases, with zero centrebody radius assumed. The solution provides the radial loading and wake sheet velocities for given blade number, radius, and forward and rotational speeds, iterating to a required ideal power coefficient under the assumption that velocities at the blade are one-half of those far downstream in the semi-infinite wake.

In the ideal wake model, the wake sheets move normal to themselves with velocity  $v_n$  and have a pitch angle  $\phi_2$  (see insert to Fig 1), where  $\phi_2 = \tan^{-1}[(V+w)/\omega r]$ . Here,  $w$  is the displacement velocity, the velocity with which the sheets move downstream as apparently rigid screw surfaces. The light loading assumption of Goldstein is anomalous in that the displacement velocity is not included in the wake geometry definition. However, the more correct solution for the radial loading, when the displacement velocity is included in the wake geometry definition, can be obtained directly from the light loading solution at the same wake pitch angle, as pointed out by Theodorsen<sup>(2)</sup>. Lock<sup>(3)</sup> took advantage of this fact in implementing Goldstein's solution by assuming a wake pitch angle equal to  $\phi$ , the onset flow angle at the blade line. This was an improvement on the infinitely light loading assumption. Lock also interpolated and extrapolated Goldstein's loading function to cover blade numbers up to six.

A method has been developed at ARA<sup>(4)</sup> to provide a numerical solution to Goldstein's formulation with the full displacement velocity included in the wake helix definition, referred to as a heavy loading model. A

solution for an arbitrary number of blades with non-zero centrebody radius is obtained. The improved representation of such features is relevant to more advanced, highly loaded propellers. Ref 5 should be consulted for an outline of the numerical scheme and a discussion of the ideal wake solution.

In order to use the method for practical propeller calculations, the strip theory approach of assuming isolated blade elements is used, following Lock<sup>(3)</sup>. Blade element onset flow conditions are linked to conditions in the far wake according to the blade element force and velocity diagram, Fig 2. The interference velocity  $w_1$  at

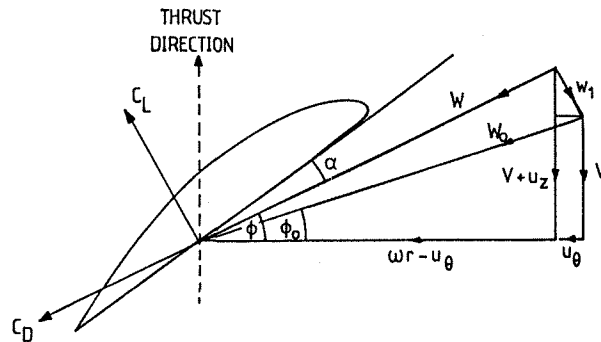


FIG. 2 BLADE ELEMENT FORCE AND VELOCITY DIAGRAM

the blade element is usually taken as one-half of the value  $v_n$  normal to the wake sheet and directed normal to the onset flow velocity  $W$ . For a given propeller planform, the loading obtained from the ideal wake solution may be converted to a lift coefficient  $C_L$  according to the local chord and onset flow conditions. The corresponding aerodynamic incidence  $\alpha$  and drag coefficient  $C_D$  may be taken from two-dimensional test data for that section. The twist is given by adding  $\alpha$  to  $\phi$  for each section across the blade. The resulting blade has an ideal loading distribution and is often referred to as an 'optimum' or minimum induced loss, design. For the true twist, usually non-optimum, it is assumed that the perturbations to the ideal loading and the interference velocity  $w_1$  at a given radial station are linearly related. New values of  $\alpha$  and  $\phi$  corresponding to the true twist are arrived at after a series of iterations, requiring the variation of  $C_L$  and  $C_D$  with incidence. Thus the method is used in conjunction with an aerofoil data bank giving  $C_L$  and  $C_D$  over ranges of geometry, Mach number and incidence. The solution may be obtained for a given blade angle, or the blade angle adjusted through several iterations until a given power coefficient is obtained. Note that although the method provides a means of determining the geometry of a blade with 'optimum' loading, the twist for maximum overall efficiency is usually determined by minimising drag losses, particularly for high speed propellers.

Various types of aerofoils are used on propeller blades. The ARA-D aerofoil series<sup>(6)</sup> is used at ARA/Dowty Rotol for lower speed applications such as commuter aircraft propellers, and derivatives of these aerofoils are used for higher speed applications. Recent work at ARA has concentrated on designing aerofoils optimised for cruise conditions on high speed propellers. These types of aerofoil are defined as families, as for NACA series 16, with simple variations of thickness and camber and with data banks available to cover a wide range of geometry and flow conditions. Experimental and theoretical investigations of the high speed aerofoil designs have been carried out to ensure acceptable data bank representation. This is particularly difficult for the thin, low camber aerofoils typical of the outer part of

the blade due to the wide range of operating conditions, from low Mach number stall at take-off to supersonic flow at cruise. The definition of families of aerofoils with associated data banks is believed to be essential for propeller applications, for example to carry out parametric studies of propeller performance for design optimisation purposes.

### Extension of the Strip Theory to Contra-Rotation

To adapt the above method for contra-rotation, the approach follows that of Lock<sup>(7)</sup>, but with an allowance for the gap between the blade rows. An ideal wake solution corresponding to half the required total power is assumed to apply independently to each rotor. The onset flow velocities at any blade element of each blade row are calculated with the inclusion of the velocity field of the other blade row. The front rotor is assumed to be affected solely by the induced axial velocity of the rear rotor  $u_z^R$ , and the rear rotor is affected by both the induced axial  $u_z^F$  and swirl  $u_\theta^F$  velocities of the front rotor, see Fig 3.

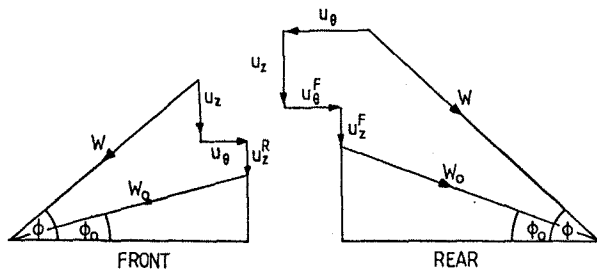


FIG. 3 BLADE ELEMENT VELOCITY DIAGRAMS FOR CONTRA-ROTATION PROPELLERS

The swirl velocity downstream of the disc plane of a rotor is assumed to remain constant, Fig 4. The induced axial velocity increases continuously through the disc plane, from a value of zero infinitely far upstream to a maximum value infinitely far downstream which is twice that at the disc plane, Fig 4. An approximation to the

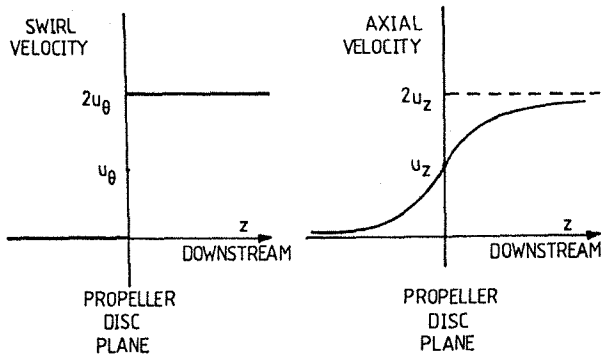


FIG. 4 INDUCED VELOCITIES ALONG AXIS

axial variation is given by an expression for the induced velocity along the axis of a semi-infinite helical vortex filament, as suggested by Aljabri<sup>(8)</sup>. Using this approach, the induced axial velocity is given in terms of the velocity at the disc plane by the following expression:-

$$u_z(z) = u_z \left[ 1 + \frac{z/R}{\sqrt{1+(z/R)^2}} \right], \quad (1)$$

where  $z$  is the distance measured downstream from the disc plane. The swirl velocity  $u_\theta^R$  imposed on the rear rotor is simply given by the constant value downstream of the front rotor, taking the circumferentially averaged value at a given radius. The axial velocity imposed by each rotor on the other is given by equation(1), taking  $z$  as the distance of separation between the blade rows. Again, the circumferentially averaged value at a given radius is used.

The solution procedure for contra-rotation propellers follows that for single rotation. Each blade row is considered in turn, with the velocities imposed by the other rotor included in the onset flow. The blade angles are adjusted during the course of the iterative sequence to give an even power split between the two blade rows, or the solution may be obtained at a specified blade angle for each blade row. Note that the validity of the contra-rotation flow model as described is open to question but it is not yet clear how it could be improved.

### Representation of Finite Blade Effects

Strip theory requires modification to account for certain features that occur on a finite rotating blade, and these can be particularly significant for high speed propellers. Towards the root there could be a flowfield perturbation due to the shape of the spinner/nacelle, and a cascade effect due to the proximity of the blades to each other. Towards the tip there is a tendency for the flow to depart from two-dimensional conditions.

The effect of spinner/nacelle shaping may be calculated to first order by a method which predicts the flowfield about a body of revolution, for example that described in Ref 9. The effect is introduced into the strip theory as a perturbation  $\Delta V$  to the freestream velocity  $V$  across the blade radius. A substantial reduction in blade onset Mach number towards the root can be obtained by appropriate shaping of the spinner/nacelle, as sketched in Fig 5. This can be an important factor in reducing drag losses in high speed cruise conditions.

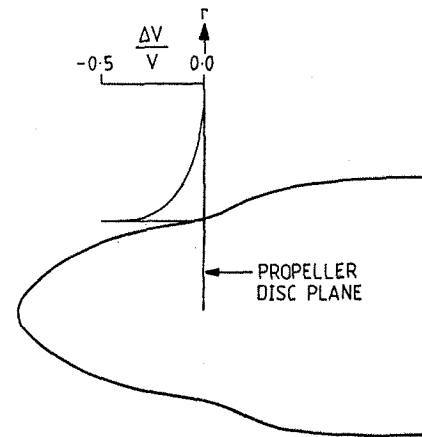


FIG. 5 EFFECT OF SPINNER/NACELLE SHAPING ON THE FLOWFIELD,  $M=0.72$

The cascade effect, at a given radial station and sectional onset Mach number, on a propeller blade is dependent on the gap and stagger distance between the blade sections, as illustrated in Fig 6. The cascade effect changes the pressures on the section, resulting in changes in lift and drag compared with the isolated section values. In order to introduce the effect into the strip theory, corrections to the data are required at the inboard radial stations and these would differ for each flow condition. Simple, easily applied corrections

are required, and the approach normally used with the advanced strip theory is to modify the lift curve slope and zero lift angle only, relative to the single aerofoil case, on the basis of subcritical, inviscid calculations by the method of Ref 10. For high Mach number and high blade number cases cascade effects can be large, and the accuracy of such simple corrections may not be sufficient. However, it is believed that three-dimensional effects are also significant for such cases, and so it is preferable to go to a fully three-dimensional theory rather than to use more sophisticated two-dimensional corrections.

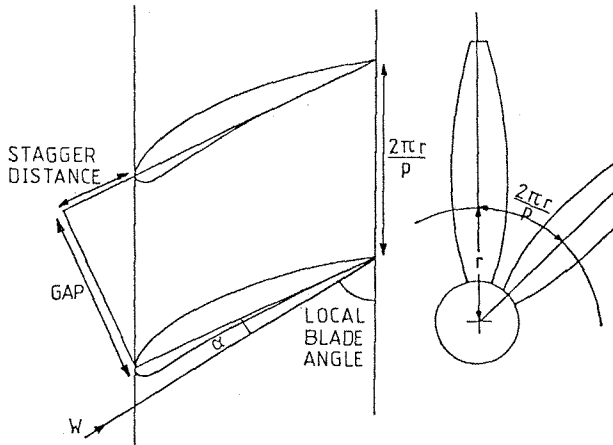


FIG. 6 AEROFOIL GAP AND STAGGER DISTANCE FOR CASCADE CALCULATION

The trend to a departure from two-dimensional flow towards the tip is allowed for in the strip theory by a tip relief correction. This gives reduced effective sectional thickness and camber towards the tip compared with two-dimensional conditions, as outlined in Ref 5. The net result is a reduction in loading towards the tip and also a reduction in drag losses for sufficiently high tip Mach number cases.

**Improved Single Rotation Wake Model**

The assumption of a regular screw surface in the far wake, of the same diameter as the propeller, is probably adequate for lightly loaded cases but for heavily loaded cases wake contraction and pitch variations could be significant, particularly just downstream of the disc plane. An investigation has been carried out at ARA into methods involving calculation of the induced velocity field due to the vortex filaments comprising the wake sheets, using the Biot-Savart law. A completely free wake analysis could have been attempted, in which the vortex filaments are allowed to move to their equilibrium positions. However, such a method would have a high computational requirement and contain many more approximations in the flow model than a fully three-dimensional Euler method, for example. Instead a simplified model in which the wake geometry is constrained has been considered.

The method calculates the velocity field due to a wake which varies in pitch and radius in the vicinity of the disc plane and develops into an ideal wake further downstream. The wake model assumed is shown in Fig 7. The method uses an input radial variation of loading for the calculation of vortex strengths across the radius. The far downstream wake is defined by an ideal wake solution according to the advanced strip theory. The method uses the radial loading given by this solution over the whole wake, including the non-regular region. The wake

contraction is determined by calculating the radial velocity at the edge of the wake sheets induced by the vortex filaments, and integrating this from the disc plane to far downstream. The pitch variation is based on the velocity variation given by equation(1). The wake geometry is recalculated during the course of the iterations until convergence is achieved.

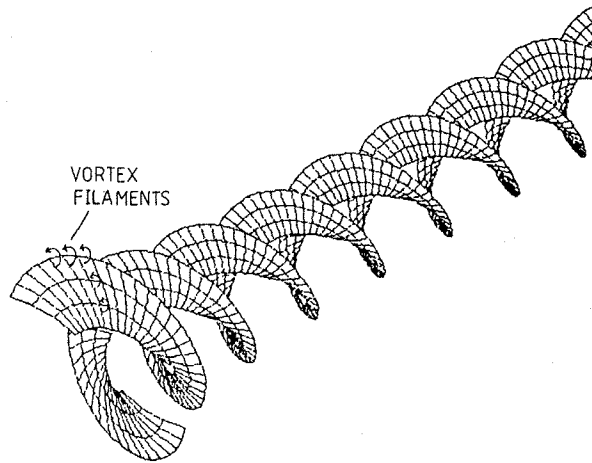


FIG. 7 VARIABLE PITCH AND RADIUS WAKE MODEL

In evaluating the method, the first stage was to consider the limiting case of a semi-infinite regular wake downstream of the disc plane, with zero pitch variation and no contraction. Check calculations showed a very close match of the flowfield between the far downstream sheets with that given by the advanced strip theory, and confirmed that the velocities at the blade line were one-half of those in the wake, as reported in Ref 5. For the regular wake case, a first-order approximation to wake contraction is given by calculating radial velocity at the edge of the sheet and integrating this from the disc plane to far downstream. An extensive range of such calculations was performed for different configurations and flow parameters, and the results were correlated as shown in Fig 8. The correlation supersedes that given by

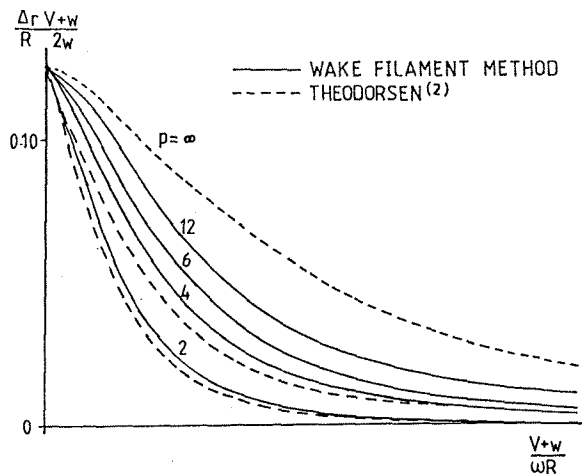


FIG. 8 WAKE CONTRACTION COEFFICIENT FORMULATION, REGULAR WAKE

Theodorsen<sup>(2)</sup>, with the advantages of being valid for any number of blades and expressed in a heavy loading form. To establish whether the first-order approximation was adequate an extensive range of calculations of wake contraction was also carried out with the full pitch and radius variations. It was found necessary to use a different form of correlation of the contraction values, treating each blade number separately. An example of the correlation for the four blade case is shown in Fig 9. The above correlations are included in the advanced strip theory, to give two options on the wake contraction for a given operating condition. The effect of wake contraction on the strip theory calculation of performance can be significant in certain conditions.

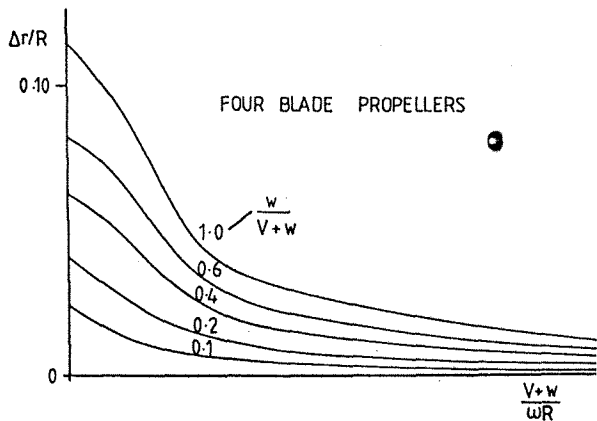


FIG. 9 WAKE CONTRACTION FORMULATION, VARIABLE PITCH AND RADIUS WAKE

The differences between the two correlations can most easily be seen by considering near-static conditions where  $V$  is small and the maximum contraction occurs. In this case, the contractions given by the constant pitch and radius and the variable pitch and radius correlations are about 20% and 10%, respectively. Whichever correlation is used, the contraction reduces rapidly with increasing forward speed to a value of only one or two per cent at cruise, even for propellers with very high disc loading. The variable pitch and radius correlation is presumably the more valid but the levels of contraction are less than might have been expected. Further validation of the wake model, either theoretical or experimental, would be desirable.

The velocity ratio at the blade line relative to the downstream wake may be calculated using the variable pitch and radius method. This ratio is typically close to one-half across the radius in conditions corresponding to cruise but may vary significantly for cases where the wake contraction and pitch variation are large. An example of the radial variation of axial and swirl velocity ratios for a four blade case is shown in Fig 10. Such variations in the velocity ratio across the radius may be included in the advanced strip theory.

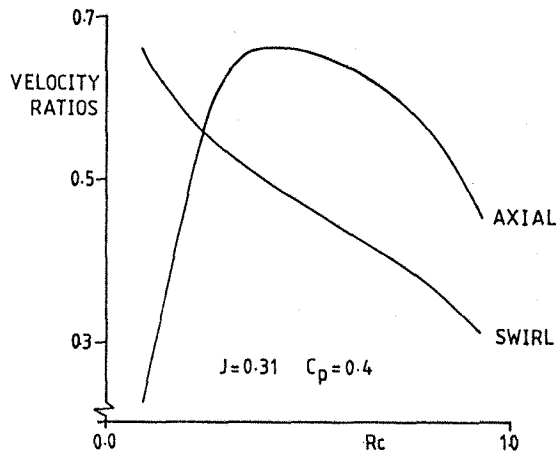


FIG. 10 INDUCED VELOCITY RATIOS ALONG BLADE LINE

### III. FIELD METHODS

#### Denton's Euler Method

A computer code developed by Denton<sup>(11)</sup> for calculating the three-dimensional inviscid flow through any type of turbomachinery blade row has been extended to apply to open rotors. This method involves the solution of the three-dimensional Euler equations using a finite volume, cell vertex, time-marching scheme. The equations are written in cylindrical polar co-ordinates, and solved in a rotating co-ordinate system using absolute quantities for all the flow variables. A variable time step appropriate to each control volume is used to accelerate convergence, and this is enhanced further by means of a simple multigrid scheme.

For propeller flowfield calculations, the method has been modified to allow a much greater distance between the blade tip and the outer boundary. The wall boundary condition at the outer boundary has been replaced by one of constant pressure, taken to be that of the freestream. The flow crossing this outer boundary is also assumed to have freestream values of density, velocity and energy, and only the flow direction is determined by the interior flow conditions. The upstream and downstream boundary conditions remain unchanged from the original turbomachinery code. Freestream stagnation pressure and temperature are assumed to apply at the upstream boundary. At the downstream boundary the radial variation of pressure is calculated assuming radial equilibrium.

The computational grid is generated algebraically and is made up of three types of non-uniformly spaced surfaces as shown in Figs 11a,b,c for a typical high speed propeller configuration. The bladewise surfaces are positioned circumferentially between the two blade surfaces. The streamwise surfaces are surfaces of revolution such that the most inboard surface coincides with the spinner/nacelle and the most outboard with the outer boundary. The quasi-orthogonal surfaces are roughly aligned with the disc plane, one containing the blade leading edge and another the trailing edge.

Due to the type of boundary conditions used it is unnecessary for the grid to extend very far upstream and downstream of the blade row. Typically, one blade radius upstream and downstream of the propeller disc plane is considered adequate. The outer boundary is generally set at a distance of two blade radii from the axis of rotation.

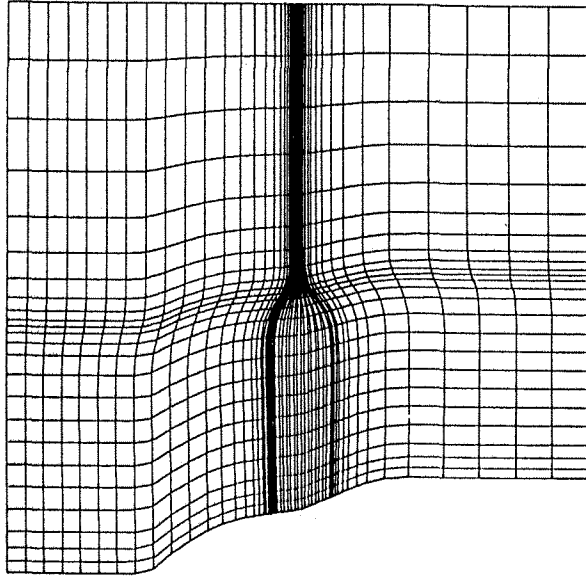


FIG. 11a GRID ON A BLADEWISE SURFACE

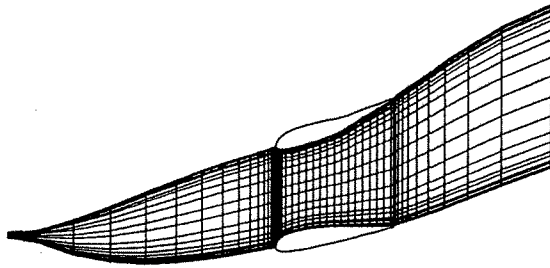


FIG. 11b GRID ON BODYSIDE STREAMWISE SURFACE  
(EXPANDED SCALE)

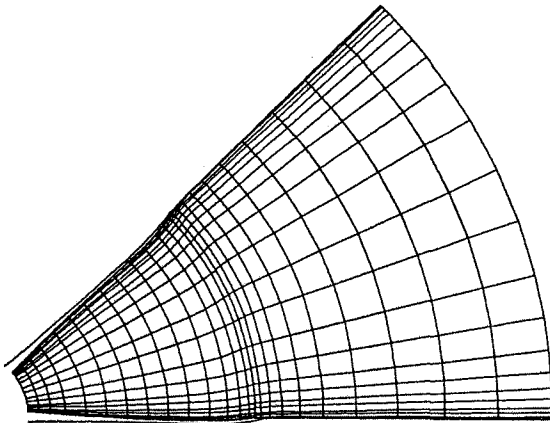


FIG. 11c GRID ON A QUASI-ORTHOGONAL SURFACE

The method is used to provide Mach number and pressure distributions throughout the flowfield and on the blade and spinner/nacelle surfaces. The blade pressures may be integrated to provide performance in terms of power and thrust coefficients. The performance calculation may include some allowance for skin friction.

## Extension to Contra-Rotation

The technique of extending the solution from single to contra-rotation propellers is the same as that described by Denton for stage calculations in turbomachines. The basic assumption is that the unsteady flow experienced by the front and rear rotors in relative motion can be approximated by the steady flow obtained when the flowfield at some axial station between the two rotors is circumferentially averaged. In this way the front rotor is presented with a circumferentially uniform downstream boundary condition whilst the rear rotor has a circumferentially uniform inlet flow. The radial variation of flow properties at the mixing plane is not specified but is a product of the calculation.

## Discussion of Modelling Issues

The Euler equations are generally considered to be an adequate mathematical model for attached compressible flow, provided that some allowance for viscous effects is made, for example by adding a boundary layer displacement thickness to the surface geometry. When applied to a single rotation propeller, solution of the steady state Euler equations with a rotational formulation is acceptable. For contra-rotation propellers the flow is inherently unsteady and, strictly, solution of the unsteady Euler equations is required. However, as this is computationally expensive, the simpler procedure outlined above is used. It should be emphasised that the circumferential averaging used is an artificial procedure designed to reduce the unsteady flow to a more manageable but possibly unrealistic steady flow.

Even when the mathematical model is acceptable, the numerical solution of the resulting equations can introduce numerous questions. Field methods require a computational grid on which to solve the equations. The number and distribution of grid points, and the positions of the boundaries of the field, all affect accuracy and possibly stability. Increasing the number of grid points should lead to a general improvement but this has to be balanced against longer computer run times and limitations on available computer memory.

An additional requirement for calculating high speed flows is that the method should capture shock waves accurately. With Denton's method, however, the pressure rise through a 'shock' tends to be spread over several grid points, that is, shock capture does not occur. This behaviour is illustrated in Fig 12, which compares local Mach numbers at around 50% radius on a typical modern propeller as computed using Denton's method and an alternative Euler method. The latter method, based on Jameson's scheme<sup>(12)</sup>, is currently under development at ARA. As Fig 12 shows, this method

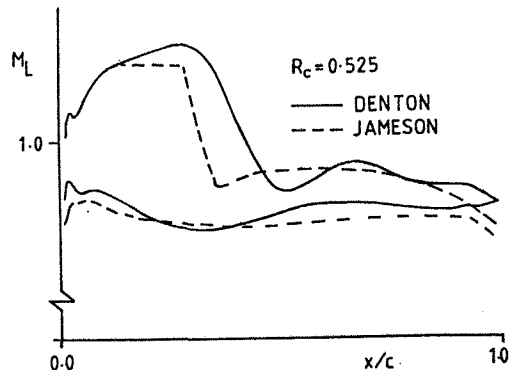


FIG. 12 COMPARISON OF SHOCK CAPTURING,  $M=0.84$

produces sharper shocks; there are also differences in shock position and other features of the surface local Mach numbers which are not yet understood.

In certain circumstances, problems also arise with solution stability in Denton's method. For example, minor changes to blade or spinner geometry can induce divergence in the solution procedure. Also, calculations at low onset Mach numbers typical of take-off conditions are usually unsuccessful. The reasons for this lack of robustness are not yet understood and a programme of investigation is currently in progress, including the development of a more general grid capability.

Denton's code is, however, reasonably easy to run, has low computer memory requirements compared to Euler codes based on Jameson's scheme, and is generally relatively quick to converge. A typical calculation for a single rotation propeller requires about 20 minutes CPU time on a Cray 1S computer and a contra-rotation case about 60 minutes. Overall, the method has proved a useful addition to the methods available for advanced propeller design.

#### IV. VALIDATION OF THE METHODS

A selection of comparisons between experimental results and predictions by the theoretical methods is given in this section. The available experimental data on high speed propellers are not yet sufficient to enable a comprehensive set of comparisons to be made with the theoretical methods. Thus comparisons for less advanced propellers at lower forward Mach numbers and with lower blade number are included, illustrating points of general relevance. The strip theory calculations include the finite blade effects and wake contraction discussed in section II. The blades considered incorporate either ARA-D or NACA series 16 sections and the strip theory calculations make use of the corresponding data banks. In the following, the strip theory comparisons are mostly of performance, with comparisons of blade loading included, and the Denton comparisons are of blade pressures only.

#### Single Rotation Propellers

##### Performance

A single rotation, eight blade, 15" (381mm) diameter model scale research propeller with ARA-D sections, designed for a Mach number of 0.72, has been tested in the ARA 9' x 8' (2.74m x 2.43m) transonic wind tunnel. The geometry of this configuration, with an untwisted planform, is sketched in Fig 13. Comparisons of experimental performance with theoretical prediction at

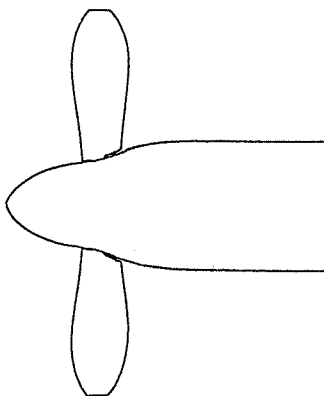


FIG. 13 RESEARCH PROPELLER GEOMETRY

$M=0.72$  are shown in Figs 14a,b,c for a number of blade angles. No information on blade deflection under load was available from the experiment. The match between theory and experiment is reasonable but is less satisfactory at higher blade angles, with an over-prediction of efficiency. Also, the variations of power and thrust coefficients with advance ratio differ between theory and experiment. There are a number of possible reasons for the differences, some of which may be related to the relatively small scale of the propeller.

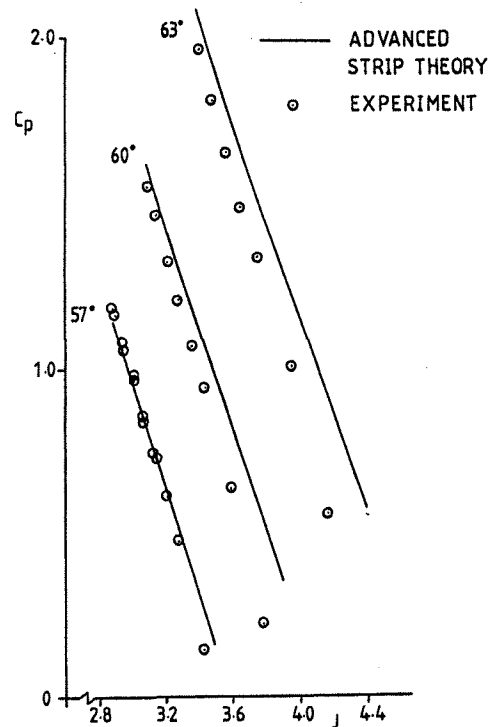


FIG. 14a POWER COEFFICIENT, EIGHT BLADE RESEARCH PROPELLER,  $M=0.72$

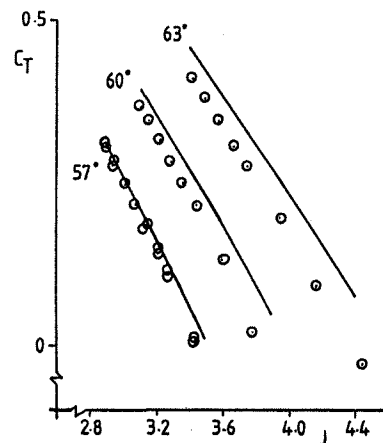


FIG. 14b THRUST COEFFICIENT, EIGHT BLADE RESEARCH PROPELLER,  $M=0.72$

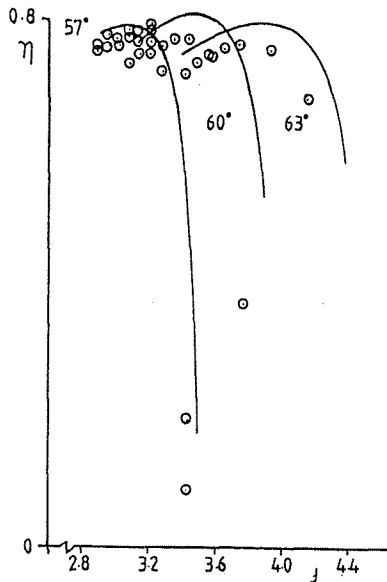


FIG. 14c EFFICIENCY, EIGHT BLADE RESEARCH PROPELLER,  $M=0.72$

Illustrations of the effects of propeller scale on power and thrust coefficients are given in Figs 15a,b. The test results are taken from experiments on full scale and one-fifth scale propellers of the type fitted to the HS748 aircraft. The propellers have four blades with NACA series 16 sections and the tests are reported in Refs 13 and 14. There are clearly appreciable differences between the full scale and model scale test results. Predictions by the strip theory are included in the comparisons and these are closer to the full scale than the model scale test results. This suggests that scale effect on the viscous layers may be a factor in the experimental differences, since the aerofoil data in the strip theory are consistent with the full scale rather than the model scale Reynolds number. However, it should be noted that the rotational speed at a given advance ratio is much higher in the model scale tests. Thus blade deflection under load and centrifugal effects on the boundary layer may differ from full scale and these factors may also need to be considered in accounting for the experimental differences.

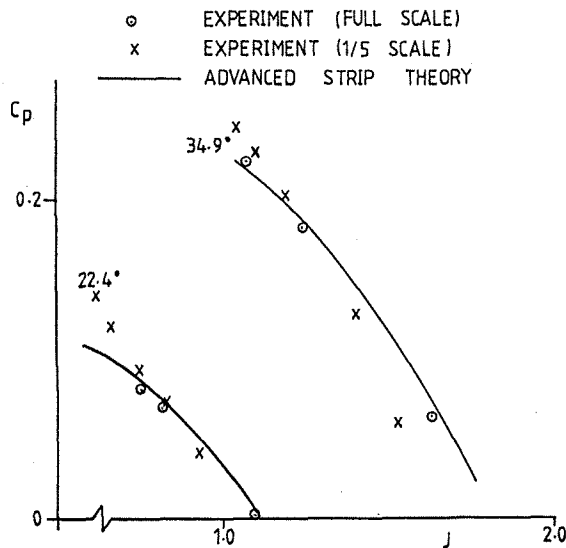


FIG. 15a POWER COEFFICIENT, HS748 PROPELLER,  $M=0.15$

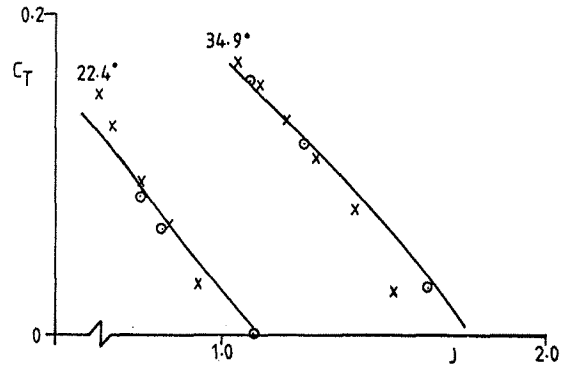


FIG. 15b THRUST COEFFICIENT, HS748 PROPELLER,  $M=0.15$

### Blade Loading

Wind tunnel measurements of blade normal force coefficient distributions from an early NACA test series on propellers with pressure tapped blades<sup>(15)</sup> are compared with the lift coefficient distributions given by the advanced strip theory in Fig 16. The propeller was large, 10' (3.05m) in diameter, and had two blades of rectangular planform comprised of NACA series 16 sections. A sketch of the geometry is included in Fig 16. In the experiment, the pressures were non-dimensionalised by the helical onset flow parameters at a given radius, and integrated to give the normal force coefficients. In this comparison, differences due to the use of lift coefficient in the theory and normal force coefficient in the experiment would be negligible. The comparison shows generally good agreement between experiment and theory when the measured blade deflection under load is included in the theoretical geometry. The figure also shows the effect of not including the tip relief correction in the calculation.

— ADVANCED STRIP THEORY ( $C_L$ )  
 - - - " " " " - NO TIP RELIEF  
 - - - " " " " - NO BLADE DEFLECTION  
 ○ EXPERIMENT ( $C_n$ )

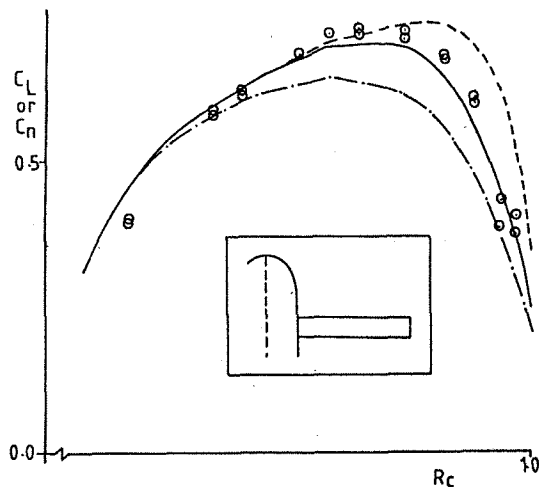


FIG. 16 LOADING DISTRIBUTIONS, NACA 10-(3)(066)-03 PROPELLER, RPM=1500,  $J=2.0$ ,  $M=0.45$



### Blade Surface Pressure Distributions

Experimental pressure distributions on the NACA blade described in the previous section are compared with those predicted by the Denton Euler method in Fig 17. In the theory, viscous effects were crudely represented by slightly modifying the section profiles to simulate the addition of the boundary layer displacement thickness. Blade angle was matched, with an allowance being made in the geometric twist for the blade deflection under load. Generally, the theoretical results are in reasonable agreement with the experiment. In detail, the prediction around the leading edge deteriorates towards the tip, probably because the grid density defined by the blade-to-blade surfaces is relatively coarse for this two blade case.

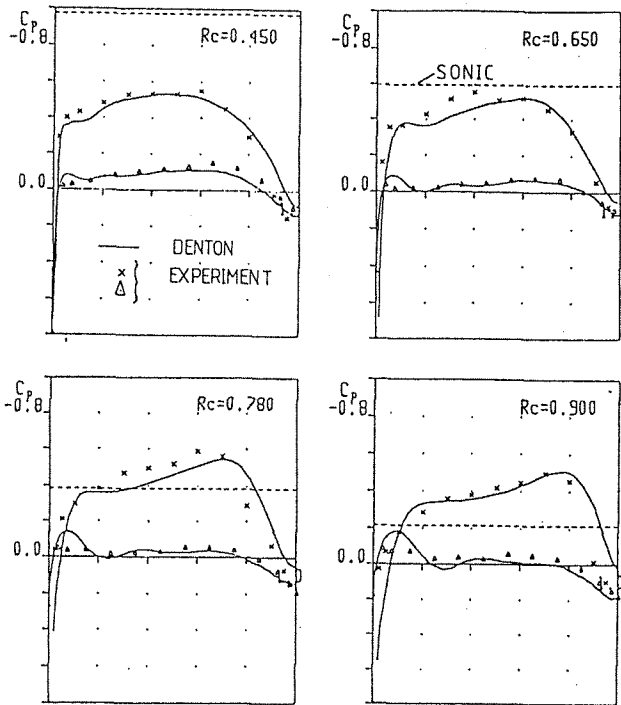


FIG. 17 PRESSURE DISTRIBUTIONS, NACA 10-(3)(066)-03 PROPELLER, RPM=1630, J=2.3, M=0.56

Experimental surface pressure distributions have been obtained at various radial stations of a two blade pressure tapped research propeller, of somewhat similar blade geometry to the propeller sketched in Fig 13. The propeller was of 24" (610mm) diameter and made of composite materials. The tests were carried out in the RAE 8' x 6' (2.43m x 1.83m) pressurised wind tunnel. The amount of blade deflection under load was not measured in the experiment, and therefore could not be allowed for in the theoretical calculations. A comparison of experimental and theoretical pressures given by the Denton Euler method and by the two-dimensional V GK method<sup>(16)</sup> at one operating condition is shown in Fig 18. The results given by the Denton method were calculated at the experimental blade angle without an allowance for viscous effects in the specified geometry. The onset flow conditions used in the V GK calculations for the sections at the various stations were obtained from an advanced strip theory calculation at the experimental blade angle.

The comparison between experiment and either theory is reasonable, but the experimental scatter is such that it is not possible to say for certain which theory is the

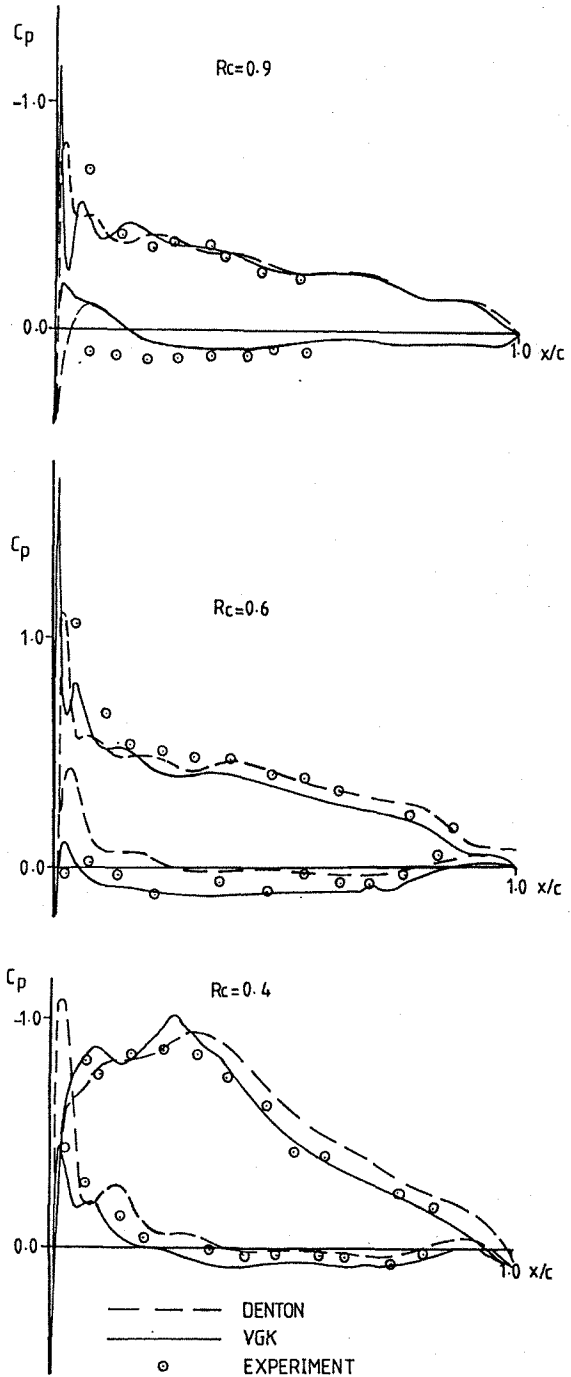


FIG. 18 PRESSURE DISTRIBUTIONS, TWO BLADE RESEARCH PROPELLER, RPM=5560, J=3.4, M=0.57

more accurate. The waviness in the pressure distributions is a consequence of the non-smooth surface geometry of the manufactured blade, which was represented reasonably closely in the calculations. The surface waviness and the limited number of chordwise pressure stations, especially at Rc=0.9, resulted from problems in manufacturing such a small size blade with embedded pressure tubes from composite materials. These problems are being addressed with subsequently manufactured blades.

# Contra-Rotation Propellers

## Performance

In the contra-rotation case, there is greater uncertainty as to the accuracy of the theoretical flow models assumed and of the experimental data than for single rotation, and hence validation of the methods is even more important. Access to modern test data of high accuracy, with measurements of the detailed flowfield, is particularly necessary for contra-rotation cases. Such tests are being carried out in the UK but the availability of the data is not yet such that comparisons with theory can be shown here. Instead, a comparison will be shown involving experimental data taken from the very limited selection available in the open literature. The data are taken from tests carried out on 3 x 3 and 4 x 4 blade contra-rotation propellers with NACA series 16 sections, as reported in Ref 15. The power coefficients for the two blade rows and the total efficiency over ranges of advance ratio at  $M=0.4$  and  $M=0.7$  for the 3 x 3 case are compared with predictions by the advanced strip theory in Figs 19a, b. At both Mach numbers the power coefficient comparisons are unsatisfactory at higher advance ratio and there is a marked over-prediction of efficiency at  $M=0.7$ . The breakdown of thrust coefficient between the blade rows was not measured and so it was difficult to go further in analysing the results to determine possible reasons for the differences between experiment and theory. This is an illustration of problems which have arisen in validating

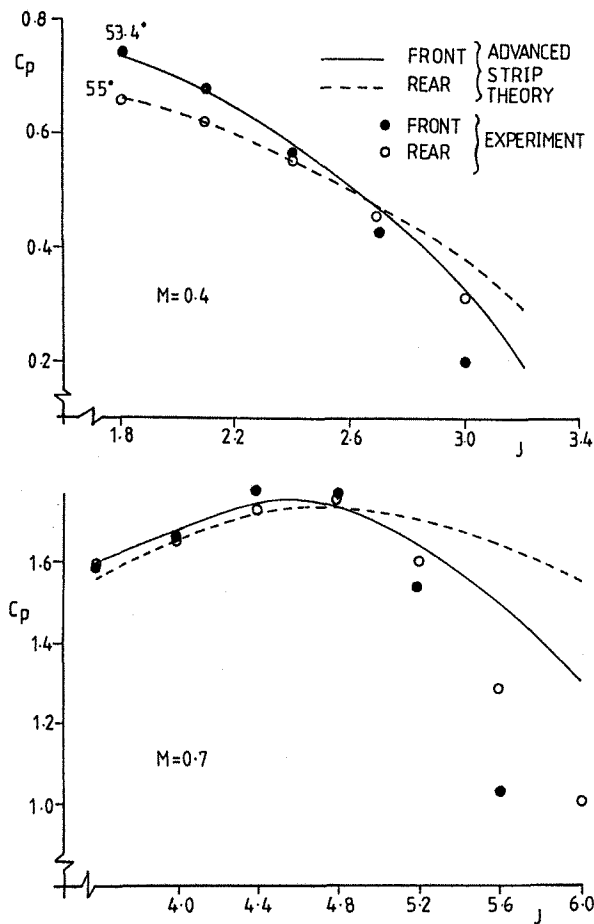


FIG. 19a POWER COEFFICIENTS, NACA 4-(5)(05)-037 3 x 3 BLADE CONTRA-ROTATION PROPELLER

the theory against early test data, for contra-rotation cases in particular. In such comparisons, the accuracy of the experiment and the validity of the theory could both be in doubt.

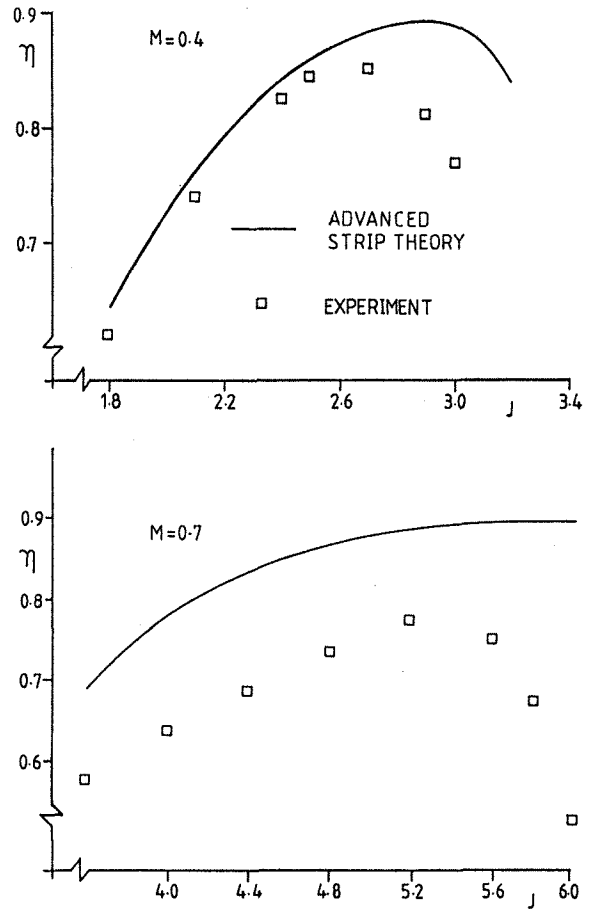


FIG. 19b TOTAL EFFICIENCY, NACA 4-(5)(05)-037 3 x 3 BLADE CONTRA-ROTATION PROPELLER

## V. APPLICATION OF THE METHODS

Two examples of use of the methods in calculations involving advanced high speed propellers are given in this section.

### Performance Analysis for a Single Rotation Propeller

In wind tunnel experiments, the performance of a propeller may be determined by measuring the forces with shaft and floor mounted balances. The general arrangement of a typical propeller test rig is shown in Fig 20. The blades and spinner are mounted on a rotating shaft and the entire configuration is supported by means of a strut. This strut must be protected from the external flow by an earth mounted shield to prevent the propeller slipstream effects on the support affecting the floor balance measurements. With this arrangement there are small gaps between the 'live' nacelle and the earthed shield, and also between the rotating spinner and the non-rotating nacelle. The floor balance measures the thrust of the entire configuration, and this must be corrected for certain tare forces associated with the strut and the shield. The torque and thrust experienced by the blades

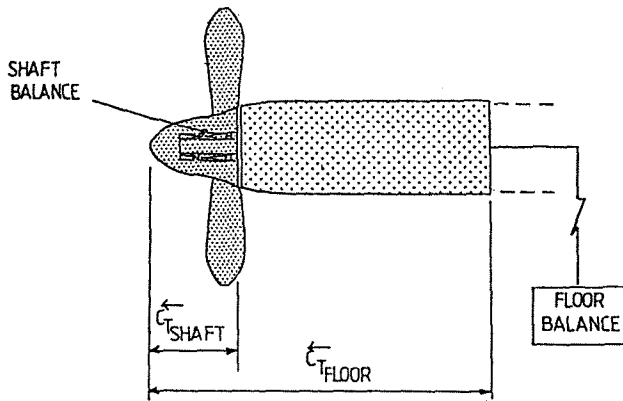


FIG. 20 FORCE MEASUREMENT FOR A TYPICAL PROPELLER TEST RIG

and spinner are measured by the shaft balance and in this case the thrust must be corrected for the spinner gap tare. Several definitions of thrust coefficient and propeller efficiency are possible from the shaft and floor balance measurements, for example the following. The difference between the shaft thrust with the propeller blades on and that with the blades off at the same freestream Mach number is called the 'apparent' thrust. The 'net' floor thrust is defined simply as the difference between the floor balance measurements for the complete configuration with blades on and blades off. Thus axial forces on the nacelle are included in the 'net' floor thrust but not in the 'apparent' thrust. Clearly the accuracy of the experimental performance figures depends not only on the reliability of the balance measurements but also on the ability to determine accurately the various tare forces.

When comparing theoretical and experimental performance results, it is not immediately apparent which definition of experimental thrust should be used. In the theoretical methods the calculation of the forces on the propeller normally includes the effect of the flowfield of the centrebody in isolation, but usually no account is taken of the effect of the propeller flowfield on the spinner and nacelle. Clearly neither of the above derivations of experimental thrust is exactly compatible with theory. By using a field method, such as Denton's Euler method, it is possible to calculate the forces on each part of the configuration separately by integrating the pressures on the blades, spinner and nacelle. Since it is also possible to use this method to calculate the flow over the centrebody alone, any of the thrust measurements according to the above definitions can be simulated. However, the results obtained from such a method do not include any allowance for skin friction. Also, with the current standard of the Denton Euler code, the centrebody radius cannot be reduced to zero. Hence, the calculated pressures around the nose region of the centrebody are unsatisfactorily defined for the purposes of accurate integration.

Work is in progress to assess the various definitions of experimental thrust using the Denton Euler method, and some results of this work are presented here. The investigation has concerned the eight blade, single rotation configuration for which results were presented in Section IV. Calculations with the Denton Euler method have been performed at  $M=0.72$ ,  $J=3.442$  for various blade angle settings. Fig 21a shows the variation of theoretical and experimental power coefficient with blade angle. Fig 21b shows the variation of the 'apparent' and 'net' thrust coefficients for both theory and experiment. Also shown is the variation of the thrust coefficient of

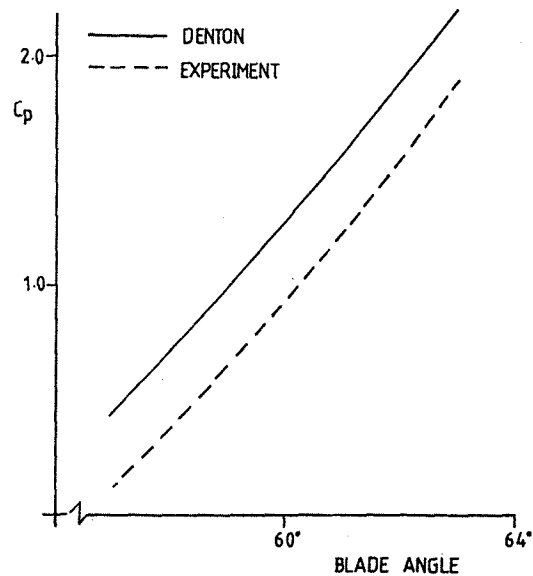


FIG. 21a POWER COEFFICIENTS, EIGHT BLADE RESEARCH PROPELLER, RPM=11000,  $J=3.442$ ,  $M=0.72$

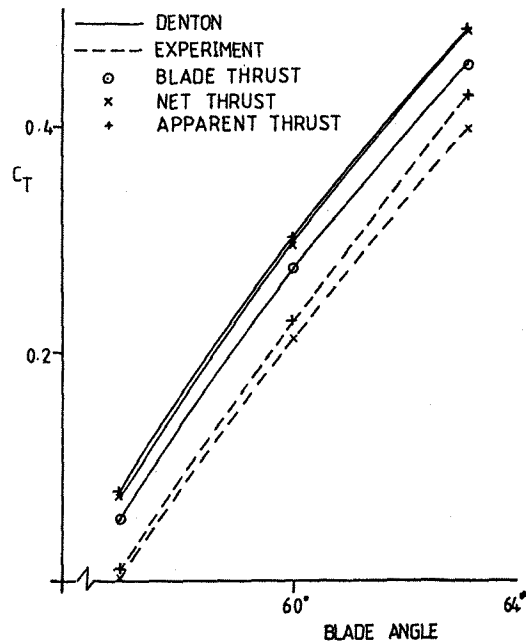


FIG. 21b THRUST COEFFICIENTS, EIGHT BLADE RESEARCH PROPELLER, RPM=11000,  $J=3.442$ ,  $M=0.72$

the blades alone as calculated by the Denton method. As can be seen the theory over-predicts both the thrust and power coefficients at all blade angles. This may be thought of as a small discrepancy in blade angle between theory and experiment, possibly attributable to the lack of viscous effects in the theory. It is apparent that the axial forces on the nacelle, indicated by the differences between 'net' thrust and 'apparent' thrust, are greater in the experiment than the theory, and increase with power. This would be expected from skin friction effects in the experiment which are absent from the theory, but may also be a consequence of detailed spinner gap flow differences in blades-on and blades-off conditions, heightened by the fact that the gap is located in the peak

suction region on the centrebody. It is also apparent from the differences between the theoretical curves that the pressure drag of the spinner is substantially reduced for blades-on conditions.

From this exercise it is apparent that considerable care must be taken in interpreting experimental performance results, especially when comparing them with theoretical predictions from either strip theory or a three-dimensional field method.

### Contra-Rotation Design

Tests on models of advanced contra-rotation propellers designed for  $M=0.8$  cruise, mostly with swept blades, are planned for the ARA 9' x 8' (2.74m x 2.43m) transonic wind tunnel. The models, with blades of 30" (762 mm) diameter, feature variations in blade number, sweep and tip speed. The untwisted planform geometry of one set of blades is shown in Fig 22. The detailed aerodynamic blade design was particularly uncertain for these configurations due to the combination of high cruise Mach number, high blade number, contra-rotation and sweep. Also, the theoretical methods had not been validated for such configurations, this being part of the aim of the tests. A three-dimensional field method would be expected to provide a more accurate description of the flowfield than the strip theory in such cases, although this is not certain. The approach adopted in the design work was to use both the strip theory and the Denton Euler method, with more reliance on the latter in the final stages. The strip theory was required for the design work to provide blade angles for the Denton calculations, as well as the variation of blade angle with power coefficient for the two blade rows.

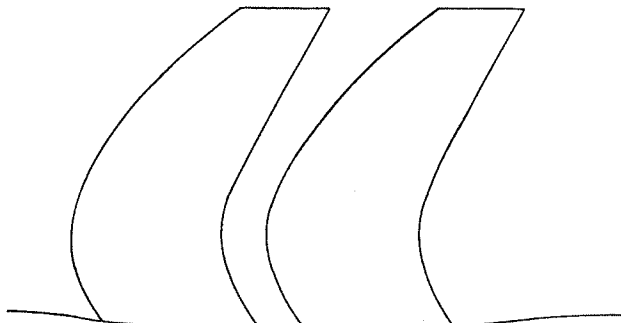


FIG. 22 SWEPT BLADE CONTRA-ROTATION PROPELLER GEOMETRY

Fig 23 shows loading distributions on the swept blades according to Denton and according to the advanced strip theory with and without cascade effects. Note that loading rather than lift coefficient has been considered in this contra-rotation case, due to the difficulty in defining equivalent helical blade onset flow conditions required to non-dimensionalise lift. The configuration had 7 x 7 blades and the calculations were performed for a forward Mach number of 0.8, tip speed of 700 ft/sec (213.4 m/sec) and equal power split. The comparisons show that the Denton loading is biased much further outboard on both rows than given by the strip theory. Use of the cascade corrections in the strip theory marginally improves the comparison, but substantial differences remain. The difference in predicted overall efficiency between the two methods was less than 2%, comparing the strip theory plus cascade corrections with Denton plus an allowance for skin friction.

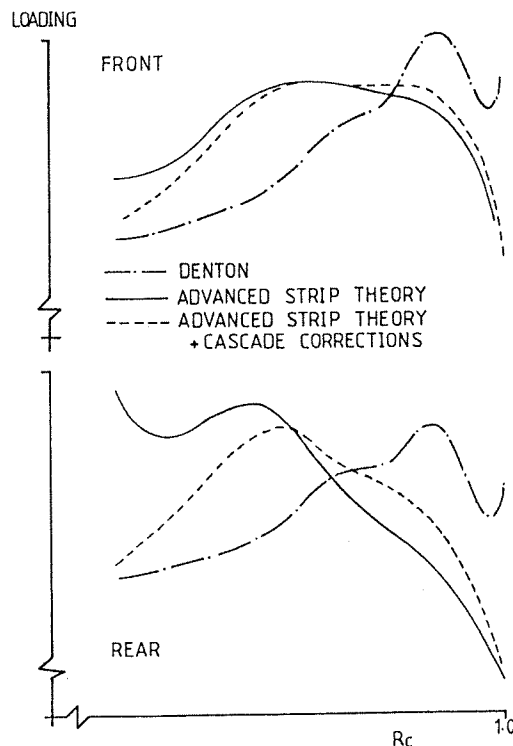


FIG. 23 SWEPT BLADE CONTRA-ROTATION PROPELLER LOADING DISTRIBUTIONS,  $M=0.8$

The differences in loading and efficiency given by the two methods were found to be similar when configuration parameters such as blade number, sweep and tip speed were varied, for a given thrust. The closeness of the performance prediction by the two, fundamentally different, methods was perhaps surprising in view of the differences in loading but gave some confidence that the performance target would be met.

Performance measurements will not be adequate to provide useful theoretical validation, and detailed flow measurements will be required. Surface pressure measurements would provide information on loading distributions but conventional techniques for surface pressure measurement present problems with such thin blades (2% thickness/chord over the outer part) and alternative techniques such as laser anemometry will be required. Such alternative techniques are planned for the test series but details have yet to be defined.

### VI. CONCLUDING REMARKS

1. Theoretical methods suitable for the prediction of propeller performance and flowfield development have been discussed, and comparisons with experiment shown. The methods discussed consist of an advanced strip theory and the Denton Euler method. Features of the methods relevant to high speed propellers with high disc loading have been emphasised.
2. The advanced strip theory has a number of additional features compared to standard Lock/Goldstein strip theory which are of particular relevance to such propellers. These features include allowances for spinner shaping, cascade effects and wake contraction, and for the spacing between blade rows in the contra-rotation case.
3. The Denton method solves the Euler equations to provide an inviscid solution for the full three-dimensional

flowfield. Allowances are required for viscous effects and, in the contra-rotation case, it is necessary to average the velocity field between blade rows to provide a steady solution. The method is reasonably robust but has certain limitations as regards detailed accuracy and solution stability, and in obtaining solutions at low forward speeds.

4. The advanced strip theory provides a reasonable prediction of the experimental performance and experimental blade loading in the single rotation cases considered.

5. The Denton method provides a reasonable prediction of blade surface pressures in the two blade single rotation cases considered, even though the method is not ideally suited to dealing with such low blade numbers due to limitations on grid density between the blade surfaces.

6. In experiments, blade deflection under load is likely and this should be taken into account in comparing with theory, if possible. The deflection may not be the same at both model and full scale and this, together with differences in viscous effects, could well influence measured performance.

7. Data from pressure tapped blades provide useful detailed validation of the theories but in the case of small scale model propellers there can be problems in manufacturing the blades with sufficient accuracy to obtain definitive data.

8. Experimental thrust measurements include contributions from the spinner/nacelle as well as the blades and different definitions of experimental thrust are possible. The three-dimensional field methods provide theoretical pressures on all surfaces and can be used to help in the interpretation of the measurements.

9. The accuracy of the theoretical methods is more uncertain for contra-rotation than single rotation due, in particular, to the need to obtain steady flow solutions by circumferential averaging of flow quantities between the blade rows. Early test data from the open literature have been found to be of limited use in validating the methods for contra-rotation. In the aerodynamic design of modern contra-rotation propellers the approach has been to use both strip theory and the Denton method. It was found that the two methods gave reasonably close predictions of performance but not of the detailed flowfield. Thus useful validation of the theoretical methods requires information on the detailed flowfield in the experiment.

## ACKNOWLEDGEMENTS

Most of the theoretical work described in the paper was carried out at ARA under contract to Dowty Rotol Ltd, partially supported by the Department of Trade and Industry. Apart from the early tests, the experiments were supported by Dowty Rotol Ltd and the Department of Trade and Industry, with partial support from Rolls Royce PLC and British Aerospace PLC in certain cases.

## REFERENCES

1. S.Goldstein, On the Vortex Theory of Screw Propellers, Proc Roy Soc A, Vol 123, 1929.
2. T.Theodorsen, Theory of Propellers, McGraw Hill, 1948.
3. C.N.H.Lock, R.C.Pankhurst, J.F.C.Conn, Strip Theory Method of Calculation for Airscrews on High Speed Aeroplanes, ARC R&M 2035, 1945.
4. J.I.Morrison, A.J.Bocci, A Numerical Treatment of the Vortex Theory of Screw Propellers, ARA MTN E26/2, 1985.
5. A.J.Bocci, J.I.Morrison, A Review of ARA Research into Propeller Aerodynamic Prediction Methods. AGARD-CP-366, 1984.
6. A.J.Bocci, A New Series of Aerofoil Sections suitable for Aircraft Propellers, Aeronautical Quarterly, Vol 28, February 1977.
7. C.N.H.Lock, Interference Velocity for a Close Pair of Contra-Rotating Airscrews, ARC R&M 2084, 1941.
8. A.J.Aljabri, The Prediction of Propeller/Wing Interaction Effects, ICAS-82-4.4.5, 1982.
9. T.J.Baker, F.A.Ogle, A Computer Program to Compute Transonic Flow Over an Axisymmetric Solid Body, ARA Memo 197, 1977.
10. M.G.Edwards, User's Guide to Multi-Aerofoil and Cascade Program (MAF), ARA Unpublished Document.
11. J.D.Denton, The Calculation of Fully Three-Dimensional Flow Through any Type of Turbomachinery Blade Row, AGARD-LS-140, 1985.
12. A.Jameson, W.Schmidt, E.Turkel, Numerical Solutions of the Euler Equations by Finite Volume Methods using Runge-Kutta Time-Stepping Schemes, AIAA Paper 81-1259, 1981.
13. W.J.G.Trebbles, Investigations of the Aerodynamic Performance and Noise Characteristics of a Dowty Rotol R212 Propeller at Full Scale in the 24ft Wind Tunnel, RAE TM AERO 2012, 1984.
14. W.J.G.Trebbles, Investigations of the Aerodynamic Performance and Noise Characteristics of a 1/5th Scale Model of the Dowty Rotol R212 Propeller, RAE TM AERO 1983, 1983.
15. J.D.Maynard, M.P.Murphy, Pressure Distributions on the Blade Sections of the NACA 10-(3)(066)-033 Propeller under Operating Conditions, NACA RM L9L23, January 1950.
16. M.R.Collyer, R.C.Lock, Prediction of Viscous Effects in Steady Transonic Flow past an Aerofoil, Aeronautical Quarterly, Vol 30, 1979.
17. J.H.Walker, R.M.Reynolds, Investigation of the NACA 4-(5)(05)-037 Six-and Eight-Blade, Dual-Rotation Propellers at Positive and Negative Thrust at Mach Numbers up to 0.9, including some Aerodynamic Characteristics of the NACA 4-(5)(05)-041 Two-and Four-Blade, Single-Rotation Propellers, NACA RM A54G13, 1954.